



**VICTORIA UNIVERSITY**  
MELBOURNE AUSTRALIA

*Smart control of BESS in PV integrated EV charging station for reducing transformer overloading and providing battery-to-grid service*

This is the Accepted version of the following publication

Datta, Ujjwal, Kalam, Akhtar and Shi, Juan (2020) Smart control of BESS in PV integrated EV charging station for reducing transformer overloading and providing battery-to-grid service. *Journal of Energy Storage*, 28. ISSN 2352-152X

The publisher's official version can be found at  
<https://www.sciencedirect.com/science/article/pii/S2352152X19310941>  
Note that access to this version may require subscription.

Downloaded from VU Research Repository <https://vuir.vu.edu.au/40971/>

# Smart control of BESS in PV integrated EV charging station for reducing transformer overloading and providing battery-to-grid service

Ujjwal Datta\*, Akhtar Kalam, and Juan Shi

**Abstract**—Uncontrolled charging demand in an electric vehicle charging station (EVCS) can potentially result in the overloading of the grid coupling transformer that will affect the transformers lifetime. This paper proposes a smart coordinated control of photovoltaic (PV) and battery energy storage system (BESS) integrated in an EVCS in order to avoid transformer overloading. BESS is designed to provide the additional EV power demand which is greater than the transformers rated capacity and thus reduce transformer overloading. In addition, the smoothing control of PV power output when PV output is lower than a threshold value is incorporated in the control method. Also, BESS which is used to provide grid services i.e battery to grid (B2G) is also incorporated in the designed smart control when the energy selling price is attractive to the BESS operator. Considering a single point connection type, B2G can only be implemented when there is no EV demand. Furthermore, B2G and battery recharging power is maintained within the transformers rated capacity to avoid overloading during their particular services. Two different sizes of BESS and transformer capacity are considered to demonstrate the overloading of transformer for a particular time of the day. A small EVCS with integrated PV-BESS in a residential area and food center is simulated to validate the efficacy of the proposed coordinated control technique. Simulation results demonstrate that the integrated BESS with the proposed control method effectively minimizes transformer overloading during all the studied network operating conditions. Moreover, BESS successfully smooths out PV power output, provide grid service and recharge the battery within the defined rated transformer capacity and thus avoids transformer overloading while satisfying design constraints.

**Index Terms**—Battery energy storage system, electric vehicle, transformer overloading, PV power smoothing, Battery to grid.

## I. INTRODUCTION

**E**LECTRIC vehicle (EV) has been expeditiously developed and adopted in the 21st century under government and manufacturers incentives, technological advancements such as larger battery capacity, fast charging and cost reductions in EV battery storage. However, the randomness of EV connection in electric power grid creates complexity in network operation and planning of the existing power system [1]. The capacity of transmission and distribution network is required to be upgraded in order to

meet the increasing demand of EV charging which requires large capital investment.

Many research studies have proposed that with an efficient planning and smart charging, the impact of EV on the grid can be minimized [2]. In order to maximize carbon dioxide (CO<sub>2</sub>) reduction, a number of studies have proposed the use of Photovoltaic (PV) system in EV charging station which can also take part in providing grid ancillary services [3], [4]. The main objective is to maximize the use of PV energy for EV charging and hence reduce the amount of purchased energy from the grid [5]. Nevertheless, the impact of PV power variation has not been given any attention while carrying out the study of integrated PV in the EV charging station (EVCS).

To tackle with the challenges of intermittent PV power and EVs load demand, various battery energy storage system (BESS) energy management techniques have been proposed in the earlier research studies [6], [7]. A stochastic pricing model is proposed in [8] to store excess energy or renewable energy when the price of electricity is low and sell back to the grid at a higher price which improves the overall profit of the charging station. The authors in [9] presented that PV-BESS in a charging station can increase the amount of annual revenue. The study in [10] presented that renewable energy and storage system reduces power consumption from the grid and hence minimizes the impact on grid. However, any clear explanation on the impact of EVCS on the grid is not available in the aforementioned [6], [8]–[11] studies. In [12], BESS is used in different operation modes, mainly to minimize peak load demand and a fixed cap for demand variation. The reduction of operation costs in a BESS integrated EVCS is studied in [13], [14], nonetheless, BESS is completely drained out in optimization process which will affect battery life [13] and no SOC constraints are considered in [14].

On the contrary, the authors in [15] presented that the certain area of a distribution network (DN), as an immediate electricity provider, can be distressed with the variable load pattern of EV. With the soaring penetration of EV, DN requires to upgrade the existing grid infrastructures to prevent power system failure due to network overloading. Many studies have been proposed on assessing the impact of EV penetration on distribution transformer. The studies in [16], [17] suggested that beyond a certain level of EV penetration, the hot-spot temperature of distribution transformer increases significantly which results in a higher loss of transformer life.

Realizing the adverse footprint of EV penetration, various methods of EV charging management and PV adoption in

This work was supported by the Victoria University International Postgraduate Research Scholarship (IPRS) scheme. The authors are with the College of Engineering and Science, Victoria University, PO Box 14428, Melbourne, Australia, 8001. Ujjwal Datta (e-mail: [Ujjwal.datta@live.vu.edu.au](mailto:Ujjwal.datta@live.vu.edu.au)). Akhtar Kalam (e-mail: [Akhtar.Kalam@vu.edu.au](mailto:Akhtar.Kalam@vu.edu.au)). Juan Shi (e-mail: [Juan.Shi@vu.edu.au](mailto:Juan.Shi@vu.edu.au)).

EVCS are recommended in the literature studies. The dynamic interaction between EV and power grid through the use of grid monitored EV charging control is presented in [18] to minimize the cost and reduce detrimental impact on the coupling transformer. A study of integrated PV in a charging station in [19] shows that this arrangement can significantly reduce overloading and hot-spot temperature of transformer during the day time with the available PV power output. Regulating EV charging as a controllable load is one of the many suggested methods that allows the reduction of peak demand resulting from EV charging [20]. This can mitigate the negative impact of EV on transformer aging and the network can sustain high EV intake with the existing infrastructure. Nevertheless, no studies have provided any insight on the capability of BESS to provide grid ancillary services (B2G) when it is not in use within the connected transformer loading capacity. Controlled EV charging is proposed in [21]–[23] by regulating EV charging in off/on-peak time [21] and slow vs fast EV charging [22] and limiting the charging power within the rated transformer capacity to avoid overloading when charging demand is higher than the transformer capacity [23]. In [24], a coordinated smart charging is proposed with PV-BESS in a charging station to reduce transformer loading. Nevertheless, the study did not consider any detailed modeling of BESS or PV and also the implementation of B2G with the installed BESS is not considered. In [25], BESS is used to reduce EV charging power demand and charging within the transformer capacity. Nevertheless, PV or B2G with the installed BESS is not studied in the work.

This paper proposes a coordinated smart charging control scheme in a PV-BESS integrated EV charging station to regulate BESS operation in such a way that the grid connecting transformer overloading can be avoided. In addition, BESS is regulated for smoothing PV power output depending on the loading of transformer and PV availability to minimize the intermittent impact of PV. Furthermore, providing grid services is also incorporated in the charging station so that BESS can sell energy to the grid within the transformer capacity limit. While BESS is delivering B2G or recharging batteries, BESS obeys the capacity limit of transformer rating.

The rest of the paper is organized as follows. Section II discusses the studied EV charging station including EV load demand profile. The modeling details of BESS control are described in Section III. The coordinated control of EV-PV-BESS in different operating scenarios are explained in Section IV. The obtained simulation results are presented and discussed in Section V and finally, the conclusions drawn are outlined in Section VI.

## II. DESCRIPTION OF EV CHARGING STATION

The arrangement of the studied EV charging station is shown in Fig. 1 where the arrows show the direction of power flow. The configuration includes a number of EVs which are connected to the main AC bus through an EV aggregator, a 22kW rated PV power source, a 200kW BESS and a grid coupling transformer. PV and BESS are connected to the main bus through their respected DC/AC converter.

The bi-directional converter allows BESS to supply and consume energy according to its control settings. Each EV is connected to the aggregator through an appropriate charging infrastructure. EV charging station is connected to the main grid via a 0.4/11kV transformer.

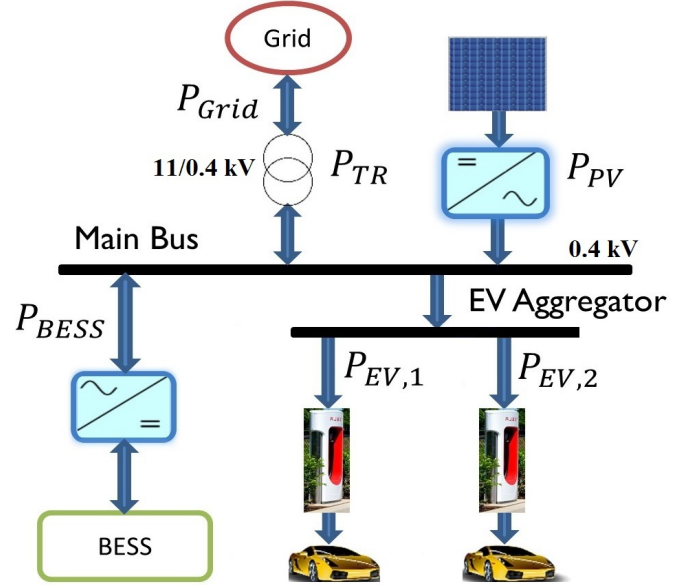


Fig. 1. Layout of EV charging station with EVs, PV and BESS

The data of EV load demand profile for two different locations, food center and residential charging load as in [26] are considered in order to calculate the required BESS power rating as shown in Fig. 2. Only the load demand which is more than 90kW is included in this study as the selected transformer capacity in this study is higher than 90kW. The load demand profile shows that the maximum load demand is 290kW for a short period of time during the whole day. This defines the probability of transformer overloading for a smaller sized transformer or over-sized capacity to avoid overloading for a shorter period of time. Hence, this study analyses the control methods and technical benefits of BESS implementation in a PV integrated EV charging station.

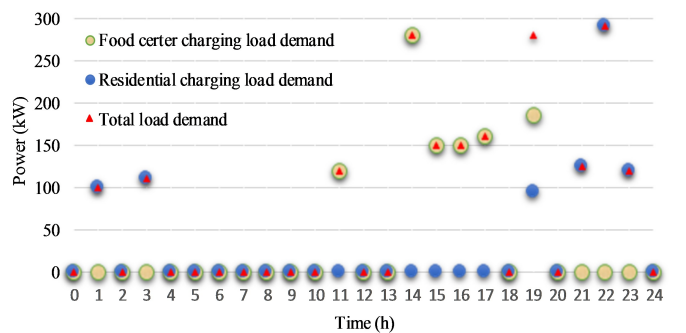


Fig. 2. Load demand profile of EV charging station in food center ( $P_{EV,1}$ ) and residential area ( $P_{EV,2}$ )

In the simulation study, instead of a detailed EV model with individual power conversion system, EVs are considered

as an aggregated active load to represent EV battery in charging mode only as in [26] and hence the randomness of individual EV battery (arrival time, initial state-of-charge (SOC), charged SOC) and EV rating are not considered. Although PV generation will vary in real time but in this study, PV is weighed to generate 20kW during the studied contingency studies. As the EV load profiles considered here are taken from the existing study, variation of EV charging demand and seasonal variation of PV are not given in-depth attention in this study. The detailed modeling is employed for BESS regulation which is discussed thoroughly in Section III.

### III. MODELING OF BESS CONTROL

The detailed BESS model comprises battery bank and a three-phase bi-directional DC/AC converter. The amount of active power support for providing various supports is constraint by battery and PWM converter capacity. Since, BESS is employed to regulate active power only, quadrature axis (q-axis) reference is set to zero and can be designed to regulate voltage. The overall BESS controller layout can be divided into the following segments:

- 1)  $P_{ref}$  generator
- 2) Active power (P) controller
- 3) Battery charge controller
- 4) d and q axis current controller
- 5) Battery model and SOC calculation

#### A. $P_{ref}$ Generator

The power reference of BESS  $P_{ref}$  generator produces the reference for regulating BESS active power according to the measured power ( $P_{meas(s)}$ ) at the transformer connection point measurements and control settings to regulate BESS active power as shown in Fig. 3 where  $P_{in}$  is the output power at BESS AC terminal. The amount of BESS power and the direction of BESS power flow varies according to its particular application. In the case of transformer overloading reduction, BESS provides the required deficit of power greater than the transformer rated capacity. The detailed measurement points and coordinated control methods for generating  $P_{ref}$  signal is discussed in Section IV for various EVCS-PV-BESS operation modes.

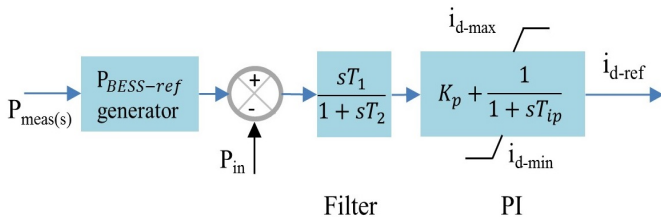


Fig. 3. BESS active power (P) controller with  $P_{BESS-ref}$  generator

#### B. Active Power (P) Controller

In active power controller,  $P_{ref}$  generates the appropriate level and direction for active power signal which is then

compared with the output power at BESS AC terminal voltage as shown in Fig. 3. The calculated power output is then passed through a first order filter followed by a PI controller that initiates current reference for direct axis (d-axis).

The first order filter considerably influences the dynamic response of the system mainly by the time constant ( $T_1$  and  $T_2$ ) values which defines slower transient response with larger time constant value. PI controller is equipped with an anti-windup limiter for avoiding integrator windup. The equation of PI controller with anti-windup [27], [28] can be written as:

$$y_o = \left[ y_{er} * \left( K_p + \frac{K_i}{T_i} \int_{y_{min}}^{y_{max}} dt \right) \right]_{y_{min}}^{y_{max}} \quad (1)$$

where,  $y_o = i_{d-ref}$  at P controller output,  $y_{max} = i_{d-max}$  and  $y_{min} = i_{d-min}$ .

The output of PI controller generates d-axis current reference ( $i_{d-ref}$ ) which is passed to the charge control. The values of PI parameters are as follows:  $K_p = 2$ ,  $T_i = 0.01$ ,  $i_{d-max} = 1$  and  $i_{d-min} = -1$ .

#### C. Battery Charge Controller

The conditions for battery charge control is shown in Fig. 4 (top) that characterizes BESS active power regulation i.e. charging and discharging action for responding to the planned events. BESS is designed to discharge if battery SOC is higher than the minimum SOC and charge if lower than the minimum SOC until it reaches to the maximum battery SOC. Nonetheless, battery charging can be adjusted depending on the energy management strategy and requirement. The minimum and maximum SOC boundary is selected as 0.2pu and 1pu, respectively which can be adjusted according to specific battery data sheet. The calculation of BESS active power regulation i.e. the control of d-axis current reference value can be expressed as follows:

$$i_{d-ref} = \begin{cases} i_{d-ref-in} & SOC \geq SOC_{min} \\ -i_{d-ref-in} & SOC \leq SOC_{max} \\ 0 & Otherwise \end{cases} \quad (2)$$

When battery SOC discharges to the minimum SOC value, it needs to be recharged. Once battery starts recharging, it will be recharged to the maximum SOC value before it can be discharged again. Battery will be recharged only if EV power demand is lower than the transformer's rated capacity i.e. the amount of BESS power for recharging is the remaining power capacity of the transformer. This will ensure that BESS does not operate in charging mode and result overloading due to battery recharging when battery SOC is at the minimum SOC and EV demand is equal or higher than the transformer capacity.

#### D. d and q axis Current Controller

The main objective of d-q axis current controller is to regulate BESS active and reactive power in response to the error between the grid reference and generated current

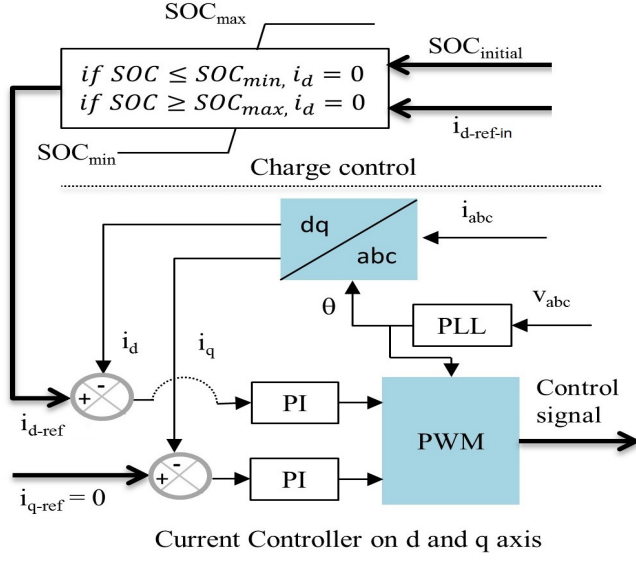


Fig. 4. BESS charge and d-q axis current control

reference. The reference for controller current input is taken from the converter's AC current in dq frame of reference through Phase-locked-loop (PLL). The output of pulse width modulation index on d and q axis provides reference phase angle to regulate DC/AC converter. As BESS is designed to regulate active power only, q-axis current is set to 0.

#### E. Battery Model and SOC calculation

The selected battery model is a simple  $R_{int}$  equivalent model which is widely utilized for dynamic studies due to its reasonable performance with simple configuration and the reduced number of parameters [29]. The battery is designed as a DC voltage source and a resistance where battery SOC and DC voltage is inversely related to each other.

The SOC of the battery is calculated according to Coulomb counting method as in (3):

$$SOC_k = SOC_{k-1} + \int_{k-1}^k \frac{\eta I_b}{3600 C_b} dk \quad (3)$$

where,  $k$  is the time in hour, the battery current and nominal battery capacity is defined by  $I_b$  and  $C_b$ , respectively. The Coulomb efficiency is defined by  $\eta$ .

## IV. REGULATION OF BESS IN PV INTEGRATED EVCS

The coordinated control is the essential part for energy management among multiple energy resources and operating conditions. This allows BESS to regulate its power flow direction to deal with the uncertainties of PV and varying load demand conditions. Each control loop is individually regulated while their inputs are somewhat dependent on each other. This ensures the operation of appropriate control loop for the particular operating condition whereas other control loop remains inactive if it is not designed to perform at that moment of time.

### A. Reducing transformer overloading with BESS

The objective of the integrated BESS is to reduce the incoming power of charging station when power demand exceeds the nominal transformer capacity. This avoids transformer overloading depending on the power output available from BESS. Hence the power at transformer can be reduced and calculated as in (4):

$$P_{TR} = \begin{cases} P_{EV} - P_{BESS} & \text{if } P_{EV} > P_{TR-nom} \\ & \text{and } SOC \geq SOC_{min} \\ P_{EV} & \text{if } P_{EV} \leq P_{TR-nom} \end{cases} \quad (4)$$

where  $P_{TR}$  is the total power demand by the transformer,  $P_{EV}$  is the total EV load demand and  $P_{EV}$  is equal to the summation of  $P_{EV,1}, P_{EV,2}$ .  $P_{TR}$  should be equal to the nominal transformer rating  $P_{TR-nom}$  to avoid overloading,  $P_{BESS}$  is the BESS power output as long as it satisfies the minimum SOC constraint. The reference for BESS power  $P_{BESS-ref}$  can be expressed as in (5):

$$P_{BESS-ref} = P_{EV} - P_{TR-nom} \quad (5)$$

The regulation of BESS for transformer overloading reduction is shown in Fig 5. When EV load demand is higher than the nominal capacity of transformer, BESS power is calculated according to (5) or else BESS power reference is zero. The generated power reference  $P_{ref}$  is then multiplied with a proportional-integral (PI) controller to produce d-axis current component as shown in Fig 3.

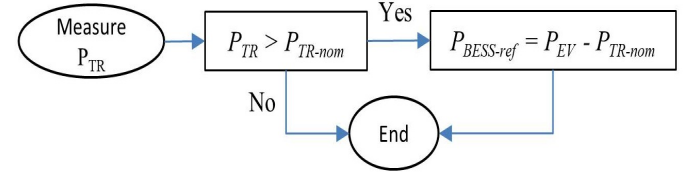


Fig. 5. Flow diagram for transformer overloading reduction with BESS

The BESS continues to provide power supply as long as battery SOC constraints are satisfied. If sufficient BESS capacity is not available during the overloading period, the total EV load demand will be fed by the grid and this will result transformer overloading.

### B. PV power smoothing and reducing transformer overloading

In order to generate and maximize sustainable energy, EVCS roof can be equipped with PV and this can help to reduce power consumption from the grid during the day time and consequently reducing transformer loading. However, PV is intermittent and with the nature of variable output over the time may affect the grid power to oscillate dramatically. The design and control of BESS in EVCS for reducing transformer overloading and PV smoothing is shown in Fig. 6. PV smoothing, in this study, is referred as supplying the deficit in PV power output than the maximum PV output.

$P_{BESS1}$  defines the amount of BESS power reference for scaling down the power feed by the transformer higher than its rated nominal value. When PV output is lower than the predefined value ( $P_{PV-lim}$ ), the power reference for BESS  $P_{BESS/PV}$  is equal to the difference between the PV power output and the predefined set value as in (6). The value of  $P_{BESS/PV}$  is zero when PV output is equal or greater than the set value.

$$P_{BESS/PV} = \begin{cases} |P_{PV} - P_{PV-lim}| & \text{if } P_{PV} < P_{PV-lim} \\ & \text{and } SOC \geq SOC_{min} \\ 0 & \text{else} \end{cases} \quad (6)$$

Since it is considered that EV power demand is always greater than the maximum PV output, BESS is not charged when  $P_{PV}$  is greater than  $P_{PV-lim}$ .

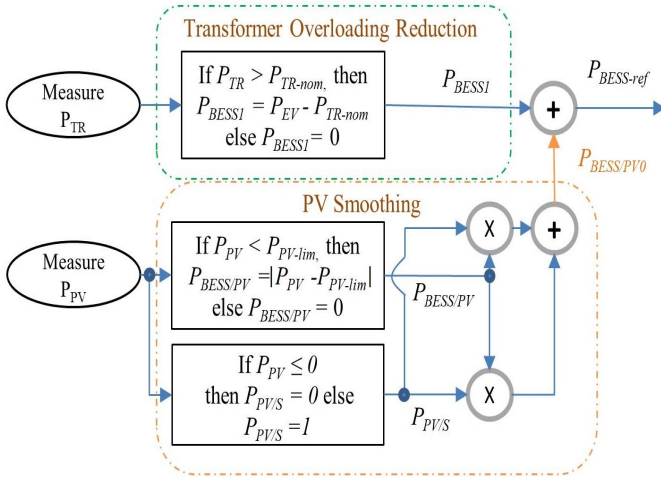


Fig. 6. Block diagram of transformer overloading reduction and PV smoothing with BESS

In order to avoid PV smoothing operation when there is no PV output ( $P_{PV} \leq 0$ ) mainly reflects night time scenario, a PV status  $P_{PV/S}$  is forwarded to the PV smoothing controller (0= not available and 1=available). A multiplier defines whether smoothing operation is needed to be active or inactive depending on the status of PV power output. The main benefit of the proposed PV-BESS coordinated control compared to the existing PV smoothing techniques is that BESS operates in smoothing control as long as PV output is available i.e. during the night time or before the sunlight, BESS will remain inactive in this control mode. This increases the efficacy of BESS control considering real life operation. Finally, BESS power reference for PV smoothing  $P_{BESS/PV0}$  is added with  $P_{BESS1}$  that generates the total BESS power reference  $P_{BESS-ref}$  for the combined operation.

### C. The coordinated control for grid service and Battery charging

The installed BESS can be utilized to sell energy to the grid (B2G) when the electricity price is high if it is allowed by the market. In this study, it is considered that BESS

participates in B2G if the price of B2G service ( $P_{B2G}$ ) is higher than the price of grid-to-battery ( $P_{G2B}$ ). It is worth mentioning that with the single power connection point, either power export or import is possible at any given point of time. BESS can be designed to provide frequency regulation if needed. The assimilated control of B2G, transformer overloading reduction, PV smoothing and battery recharging is shown in Fig. 7 (on the left column). The mode of operation is regulated by the direction of power flow. The output at BESS power reference for overloading reduction and PV smoothing  $P_{BESS-ref/OLS}$  is available if the direction of power flow is from grid to the EVCS i.e. positive or neutral. In the case of B2G implementation,  $P_{BESS-ref/OLS}$  becomes zero as the power flows from EVCS to the grid i.e. negative and thus  $P_{BESS-ref/B2G}$  regulates the BESS power reference  $P_{BESS-ref1}$ . The limit of BESS active power output for B2G ( $P_{TR-B2G-lim}$ ) is constrained within the ratio of transformer's nominal capacity ( $P_{TR-nom}$ ) and total BESS capacity ( $P_{BESS-nom}$ ) to ensure transformer overloading is avoided (when BESS size is higher than transformer rating) during B2G service periods as shown in (7):

$$P_{TR-B2G-lim} = P_{TR-nom} / P_{BESS-nom} \quad (7)$$

The generated power reference is then passed through a PI controller to generate d-axis current component and hence the maximum and minimum limit needs to be adjusted according to the service that BESS is providing. The coordinated active power (P) controller arrangement is shown in Fig. 7 (on the right column). During the operation of transformer overloading reduction and PV smoothing, BESS is regulated within the maximum and minimum BESS capacity and hence the signal  $P_{B2G/S1}$  is equal to 1. However, the employment of B2G adjusts BESS output limit within the transformer nominal capacity  $P_{TR-B2G-lim}$  and hence  $P_{B2G/S}$  is equal to 1 and  $P_{B2G/S1}$  is zero. Each operating limits are managed by their corresponding mode of operation.

Battery is designed to be recharged for two different scenarios: (1) when SOC is lower than the minimum 0.2pu or (2) when SOC is lower than 0.5pu and d-axis current reference  $i_{d-ref}$  is less than 0.0001pu which avoids recharging when battery is discharging and  $0.5pu > SOC > 0.2pu$ . To avoid transformer overloading during battery recharging, battery will recharge when  $P_{TR} < P_{TR-nom}$  and the recharging BESS power ( $P_{BESS/ch}$ ) is equal to the available transformer capacity which can be calculated as  $P_{TR} - P_{TR-nom}$ . The status of SOC  $S_{SOC}$  changes according to the aforementioned defined scenarios.

### D. BESS (kW) and Transformer (kVA) sizing

In order to select a proper size of BESS, it is imperative to determine transformer's nominal rating and BESS efficiency. According to the load demand profile of the selected area as shown in Fig. 2 which illustrates that load demand is relatively high for a particular time of the day. Two different sizes of transformer, a 121kVA and 200kVA transformers ( $P_{TR-nom}$ ) are selected in this study which explains that overloading after

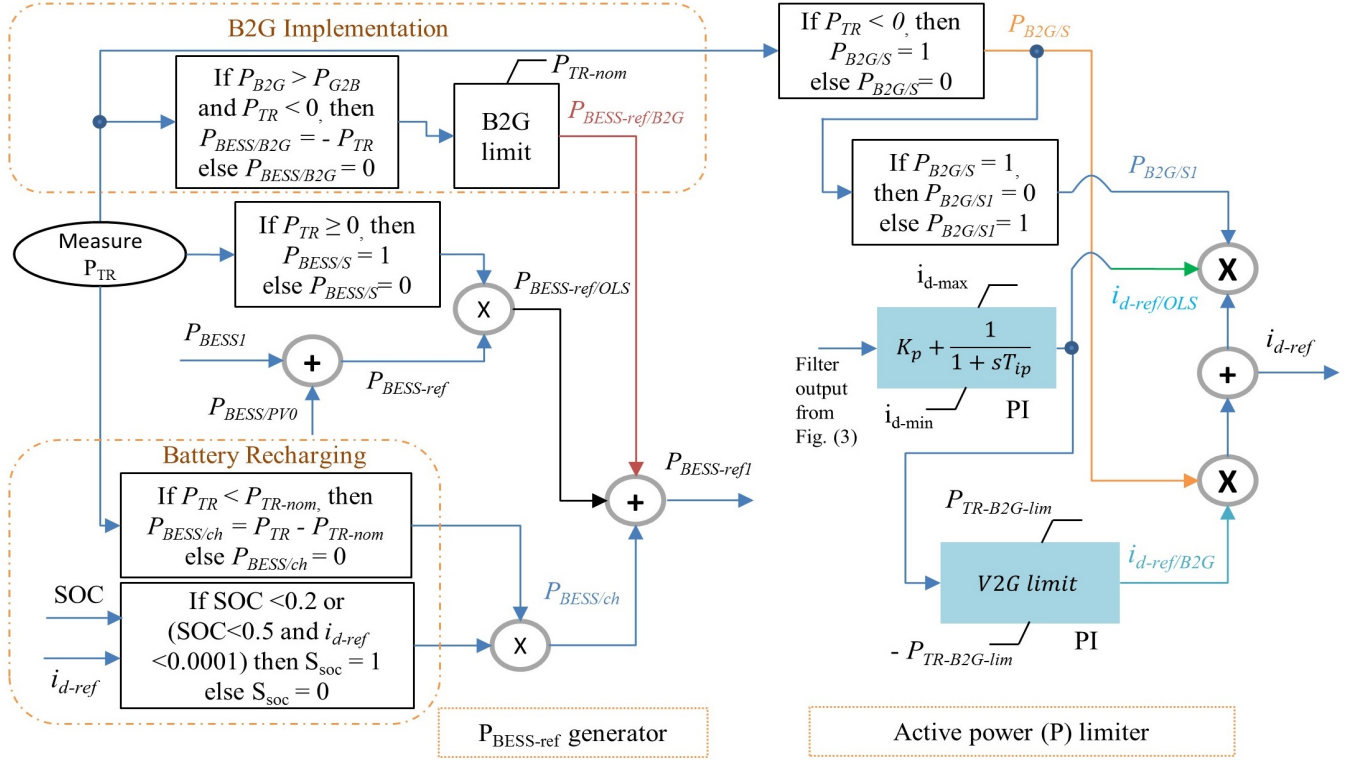


Fig. 7. Block diagram of reducing transformer overloading, smoothing PV output and B2G at EVCS with BESS

2pm until approximately 11pm can be easily avoided with the selected transformers sizes.

On the contrary, the maximum EV charging load demand ( $P_{EV-max}$ ) is 288kW at about 10pm. In order to lessen the power feed from the grid and minimize transformer overloading, the required BESS size ( $P_{BESS-req}$ ) can be calculated as in (8):

$$P_{BESS-req} = P_{EV-max} - P_{TR-nom} \quad (8)$$

In the case of 200kVA transformer, the overloading after 2pm until approximately 11pm can be easily avoided with a smaller size of BESS. In addition, this will not result an overloading of the transformer during B2G or recharging of the battery as the BESS size is smaller than the transformer rated capacity. On the contrary, with a 121kVA transformer, the required BESS size is 167kW. Hence, the required BESS size is 167kW. Assuming the charging and discharging efficiency is 85% [30], a 200kW of BESS is selected. However, it is worth mentioning that this is not an optimal size of BESS or transformer and the optimal size can be determined in the future work. The complete energy management of BESS in various operation modes are summarized in the flowchart as shown in Fig. 8.

## V. RESULTS AND ANALYSIS

The viability of the proposed coordinated control method is validated through multiple case studies and they are listed as follows:

- (a) Transformer overloading reduction with BESS and without PV
- (b) Coordinated control of PV & BESS for reducing transformer overloading and PV smoothing
  - (1) Constant PV output and transformer overloading reduction
  - (2) PV power smoothing only
  - (3) PV power smoothing and transformer overloading reduction
- (c) EVCS BESS for B2G

The model is subjected to operate in various control mode such as grid-to-vehicle (with and without PV/BESS) and B2G. Hence, it is considered that EVCS can either export or import power at any given point of time in order to achieve relatively a simple but an efficient control of BESS. Two different sizes of transformer limit is considered i.e. 121kW and 200kW in order to demonstrate the efficacy of the proposed BESS control method.

### A. Transformer overloading reduction with BESS and without PV

The EVCS charging load demand and transformer overloading with BESS is shown in Fig. 9. As Fig. 9(a) illustrates, EV load demand ranges from 95kW-288kW [26]. A 120kW is considered as typical load consumption for the simulation studies. A 87.5% increase in the load demand (225kW) at  $t = 5s$  is applied which implies 104kW to be supplied by BESS in order to avoid transformer overloading

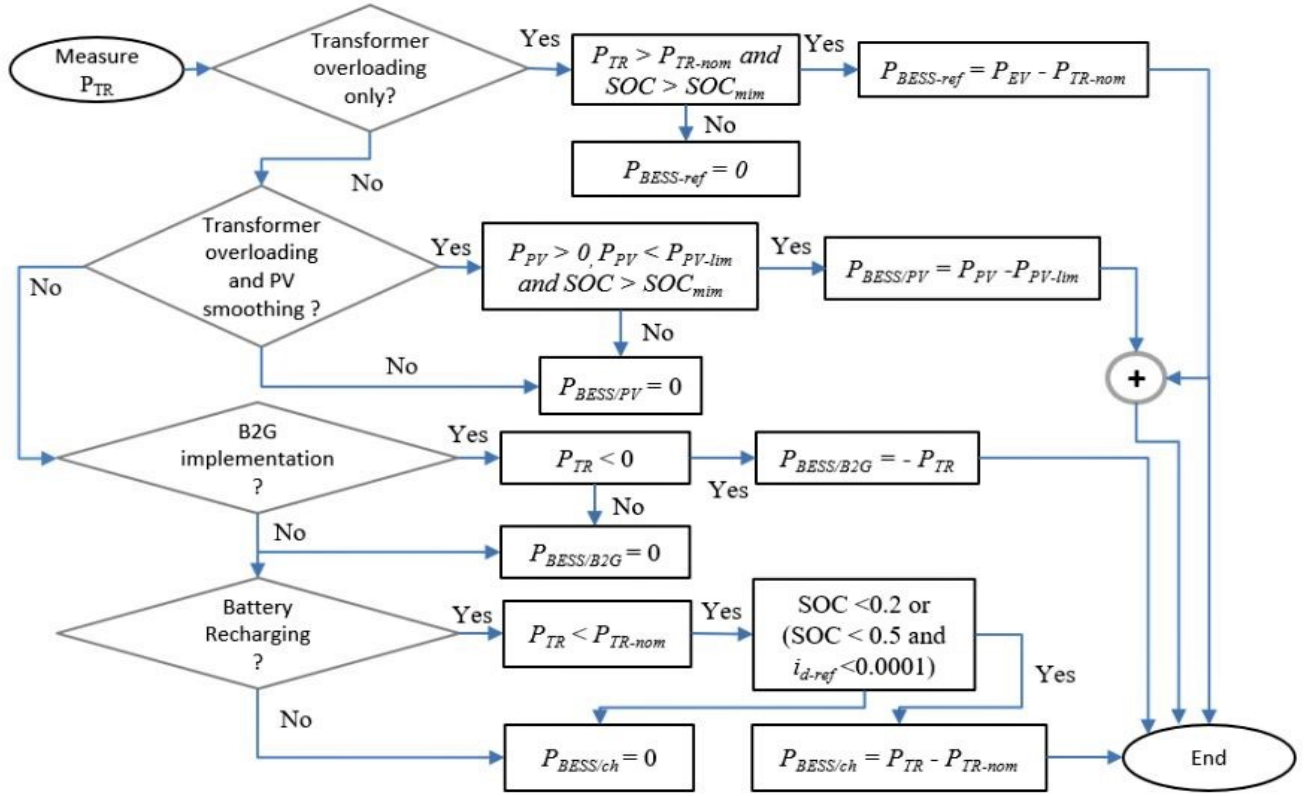


Fig. 8. Flowchart for the proposed energy management strategy under various operation modes

for a 121kVA transformer. At  $t = 65s$ , load demand is reduced to the normal condition before increasing the load demand by 140% at  $t = 70s$ . This raises BESS power demand to 167kW in order to reduce transformer overloading. When a 200kVA transformer is selected, the required BESS power output is reduced to 25kW and 88kW. Fig. 9(b) shows transformer overloading (%) in various operation modes. It can be seen that without a BESS, a 121kVA transformer is overloaded upto 238% for the studied load event scenario as shown in the Fig. 9(b). With a 200kVA rated transformer, a relatively smaller size of BESS (100kW) is sufficient to reduce transformer overloading completely. However, a deeper insight on techno-economic analysis can provide an optimal transformer and BESS size to gain maximum benefit. Nevertheless, this study is focused on the control of BESS for multiple services and hence economic analysis is out of the scope of this study. Hence, the reduction of transformer loading with the integrated BESS will decrease the rise in hot spot temperature that minimizes the negative impact of transformer loss of life as suggested in [22].

The BESS power output during the minimization of overloading is shown in Fig. 10(a). It is visible that 200kW BESS provides 104kW and 167kW according to the variable demand established by the load event and successfully cuts down transformer overloading which validates the efficacy of the proposed BESS control mode. For a higher transformer size (200kVA) and a 100kW BESS, loading at peak demand can be maintained within 100% of the nominal capacity.

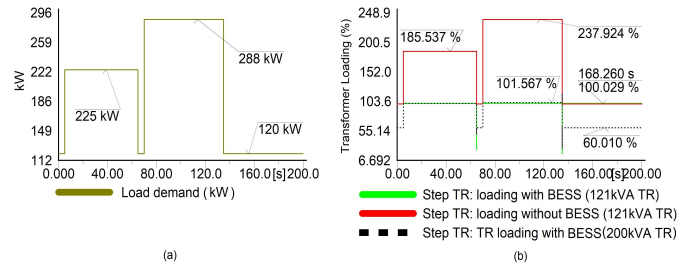


Fig. 9. EVCS load demand (a) and transformer loading condition in various modes (b)

Battery energy capacity is 1.8kWh. Battery SOC for both cases are presented in Fig. 10(b) deteriorates over the time that demonstrates the importance of BESS energy capacity to provide aforesaid services for longer periods.

### B. Coordinated control of PV & BESS

It is considered that a 22kW PV is installed in EVCS roof. Considering 20kW PV output, the power consumption from the grid is now reduced for the same load even as described in section V-A. The required BESS power for decreasing overloading is reduced to 84kW instead of 104kW (19.23% reduction) and 147kW instead of 167kW (11.97% reduction) as in the case of previous section for 200kW installed BESS due to the installed rooftop PV output. The BESS power output for this scenario is displayed in Fig. 11 (a). With 200kVA

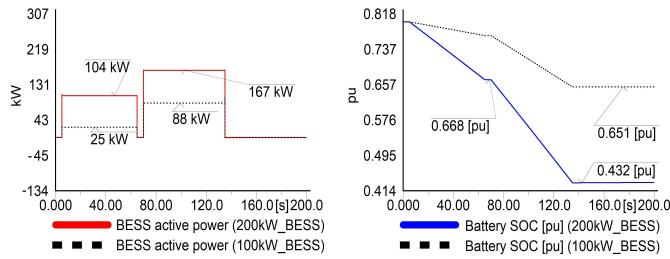


Fig. 10. BESS active power output (a) and battery SOC (b) during transformer overloading period

transformer, the required BESS power output is reduced to 5kW (225-200kW) for the duration of 60s and 68kW for  $t=70s-135s$ . Transformer overloading with BESS remains the same as in the previous case i.e. within the nominal capacity as depicted in Fig. 11 (b). However, in all other cases, transformer overloading is reduced compared to the previous case in section V-A as PV feeds a portion of the EVCS load demand and hence, in general, EV power demand from the grid is decreased.

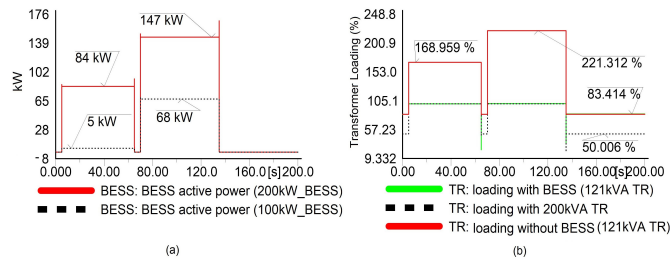


Fig. 11. BESS active power output (a) and Transformer loading (b) during overloading reduction with constant PV output

In the case of PV smoothing, it is considered that load demand is constant and below the rated transformer capacity. The BESS is designed to participate in smoothing control if PV power output drops below 20kW which is adjustable according to the designer preference. At  $t = 5s$ , PV power output is reduced to 15kW and  $t = 15s$  power output is further lessen to 13kW until  $t = 25s$  as depicted in Fig. 12(a). The BESS power output as shown in Fig. 12(b) illustrates that BESS efficaciously supplies the required power according to the designed control settings.

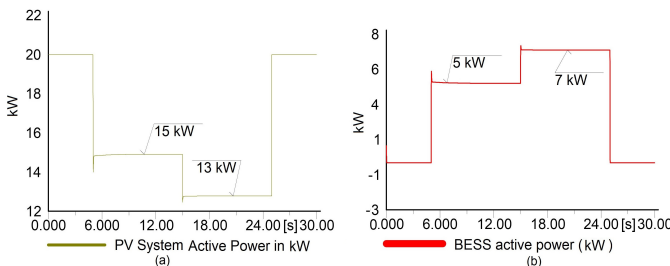


Fig. 12. PV output variation (a) and BESS active power output (b) during PV smoothing with no transformer overloading action

In order to demonstrate the amalgamated control of

PV-BESS in accordance with EVCS load demand and PV output variation as in Fig. 12(a) and load event as in Fig. 11(a) is applied. At  $t = 5s$ , the power reference of 200kW BESS for transformer overloading is 84kW and PV power smoothing is 5kW, hence the total power reference is 89kW. With the further reduction of PV output to 13kW at  $t = 15s$ , the power reference rises to 91kW. The power reference for 100kW BESS is 10kW, 12kW, 68kW respectively for the same applied contingency periods. The BESS power output as shown in Fig. 13(a) portrays that with the variation of transformer overloading and PV smoothing, BESS regulates its power output effectively while maintaining transformer overloading within the allowable limit. This characterizes the competence of the proposed PV-BESS coordinated control method for minimizing transformer overloading and PV smoothing operation seamlessly. Fig. 13(b) manifests the reduction of transformer overloading with the dynamic operating conditions that exhibits effective regulation of the proposed control method.

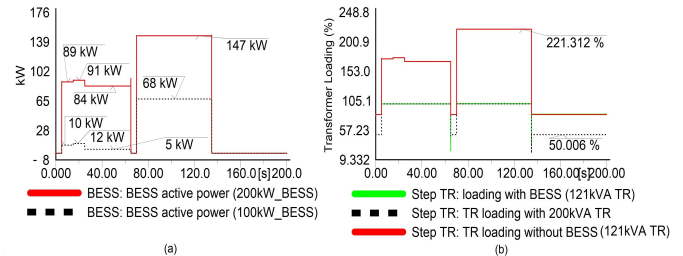


Fig. 13. BESS active power output (a) and Transformer loading (b) during transformer overloading reduction and PV smoothing

BESS should participate in PV smoothing only during the day time i.e. when PV output is available. To demonstrate the proposed feature, further simulation studies are carried out as shown in Fig. 14. BESS provides the power deficit until PV power output is greater than zero (before  $t = 25s$ ). As soon as the power output of PV reduces to zero at  $t = 25s$ , BESS stops injecting any power according to the proposed design as shown in Fig. 6.

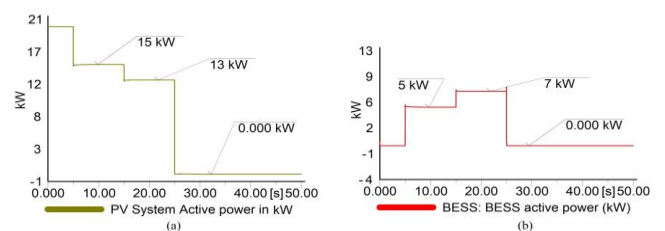


Fig. 14. PV output variation (a) and BESS active power output (b) during the night time

### C. EVCS BESS for B2G

In B2G control mode, BESS can be regulated according to the selling price of electricity when there is no charging load demand at EVCS. The grid services can be ranged to

energy arbitrage and can be further modified for frequency regulation, if needed. It is assumed that electricity price is high enough and hence EVCS agreed to participate in B2G. BESS can perform B2G operation as long as battery SOC is within the defined minimum SOC limit. In order to avoid transformer overloading during B2G operation, BESS power output is constrained by the rated transformer capacity. When B2G demand is higher than the transformer rating, BESS power output is restrained equal to the transformer rated capacity. The proposed B2G implementation with and without the above mentioned operation limit is illustrated in Fig. 15(a). A power demand of 140kW by the grid is enforced during  $t = 4s-20s$ . It can be observed that as BESS output capacity is 170kW, BESS can supply the total 140kW load demand and this results unwanted transformer overloading. However, with the confined BESS power regulation for B2G, BESS only supplies equal power to the transformer nominal capacity of 121kW and thus avoids overloading of the transformer. When a 200kVA transformer is selected, the power demand is restricted by the BESS capacity only. As expected, Battery SOC is highest for 100KW BESS as compared to 200kW as BESS discharges less power as depicted in Fig. 15(b).

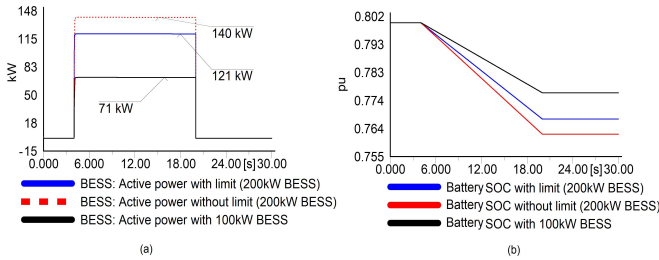


Fig. 15. BESS active power output (a) and battery SOC (b) during B2G with and without transformer overloading constraint

#### D. Battery recharging within the transformer capacity

The proposed battery recharging strategy is illustrated in Fig. 16. Fig. 16(b) suggests that battery is not recharged when battery SOC is higher than 0.5pu, as charging is not required according to the design. On the contrary, Fig. 16 (a) depicts that when SOC is 0.46pu, load demand fed by the transformer is  $141-20=121kW$  which means the transformer is already operating at its rated capacity and hence, not enough capacity (NEC) is available to charge the battery. Nevertheless, when load power demand delivered by the transformer reduces to  $92-20=72kW$ , a  $121-72=49kW$  of capacity is available to recharge the battery while staying within the transformer rated capacity. The battery continues to recharge with a power consumptions of 49kW. For 200kVA transformer, the load demand fed by the transformer is  $141-20=121kW$  and hence 79kW is available for use without being overloaded. Therefore, the battery can be charged with a power consumption of 79kW.

## VI. CONCLUSION

This study proposed a coordinated control of PV-BESS in a EVCS for reducing the overloading impact of charging

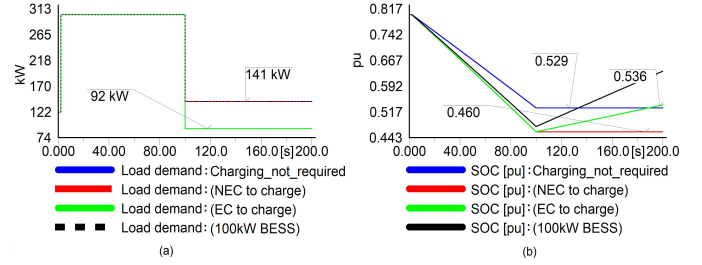


Fig. 16. BESS active power output (a) and battery SOC (b) during B2G with and without transformer overloading constraint

load demand on grid connecting transformer. The model comprises a detailed BESS design and control techniques for curtailing load demand from the grid during overloading conditions, providing PV power smoothing and B2G services. The investigation is carried out in term of technical feasibility analysis and the key summary can be outlined as follows:

- A properly sized BESS capacity can effectively reduce power consumption from the grid during the overloading periods i.e. it is shown that nearly 138% reduction in transformer overloading can be achieved depending on the size of BESS and thus transformer loss-of-life can be minimized.
- In the coordinated control of PV-BESS, BESS is capable of regulating its power output for reducing transformer overloading and PV power smoothing simultaneously depending on the requirement of EVCS. The aim is to demonstrate the controlling efficacy for various purposes that can be easily adapted to other design requirements.
- BESS participates in B2G if the energy selling price is higher than the energy consumption price by the battery.
- In B2G, constraining BESS power output to the transformer nominal rating is essential to avoid transformer overloading if the BESS capacity (200kW) is greater than the transformer nominal capacity and the proposed method successfully achieves the expected outcome. However, when a higher transformer is selected, the controller is easy to be adjusted according the updated transformer size.

## REFERENCES

- [1] J. Y. Yong, V. K. Ramachandaramurthy, K. M. Tan, and N. Mithulananthan, "Bi-directional electric vehicle fast charging station with novel reactive power compensation for voltage regulation," *International Journal of Electrical Power & Energy Systems*, vol. 64, pp. 300 – 310, 2015.
- [2] Z. Moghaddam, I. Ahmad, D. Habibi, and Q. V. Phung, "Smart charging strategy for electric vehicle charging stations," *IEEE Transactions on Transportation Electrification*, vol. 4, no. 1, pp. 76–88, March 2018.
- [3] G. R. Chandra Mouli, M. Kefayati, R. Baldick, and P. Bauer, "Integrated pv charging of ev fleet based on energy prices, v2g, and offer of reserves," *IEEE Transactions on Smart Grid*, vol. 10, no. 2, pp. 1313–1325, March 2019.
- [4] Q. Chen, N. Liu, C. Hu, L. Wang, and J. Zhang, "Autonomous energy management strategy for solid-state transformer to integrate pv-assisted ev charging station participating in ancillary service," *IEEE Transactions on Industrial Informatics*, vol. 13, no. 1, pp. 258–269, Feb 2017.
- [5] Y. Zhang and L. Cai, "Dynamic charging scheduling for ev parking lots with photovoltaic power system," *IEEE Access*, vol. 6, pp. 56 995–57 005, 2018.

- [6] M. A. Quddus, O. Shahvari, M. Marufuzzaman, J. M. Usher, and R. Jaradat, "A collaborative energy sharing optimization model among electric vehicle charging stations, commercial buildings, and power grid," *Applied Energy*, vol. 229, pp. 841 – 857, 2018.
- [7] G. Hilton, M. Kiaee, T. Bryden, A. Cruden, and A. Mortimer, "The case for energy storage installations at high rate ev chargers to enable solar energy integration in the uk an optimised approach," *Journal of Energy Storage*, vol. 21, pp. 435 – 444, 2019.
- [8] C. Luo, Y. Huang, and V. Gupta, "Stochastic dynamic pricing for ev charging stations with renewable integration and energy storage," *IEEE Transactions on Smart Grid*, vol. 9, no. 2, pp. 1494–1505, March 2018.
- [9] L. Yang and H. Ribberink, "Investigation of the potential to improve dc fast charging station economics by integrating photovoltaic power generation and/or local battery energy storage system," *Energy*, vol. 167, pp. 246 – 259, 2019.
- [10] J. Domnguez-Navarro, R. Dufo-Lpez, J. Yusta-Loyo, J. Artal-Sevil, and J. Bernal-Agustn, "Design of an electric vehicle fast-charging station with integration of renewable energy and storage systems," *International Journal of Electrical Power & Energy Systems*, vol. 105, pp. 46 – 58, 2019.
- [11] X. Han, Y. Liang, Y. Ai, and J. Li, "Economic evaluation of a pv combined energy storage charging station based on cost estimation of second-use batteries," *Energy*, vol. 165, pp. 326 – 339, 2018.
- [12] L. Novoa and J. Brouwer, "Dynamics of an integrated solar photovoltaic and battery storage nanogrid for electric vehicle charging," *Journal of Power Sources*, vol. 399, pp. 166 – 178, 2018.
- [13] Q. Yan, B. Zhang, and M. Kezunovic, "Optimized operational cost reduction for an ev charging station integrated with battery energy storage and pv generation," *IEEE Transactions on Smart Grid*, vol. 10, no. 2, pp. 2096–2106, March 2019.
- [14] H. Mehrjerdi and R. Hemmati, "Electric vehicle charging station with multilevel charging infrastructure and hybrid solar-battery-diesel generation incorporating comfort of drivers," *Journal of Energy Storage*, vol. 26, p. 100924, 2019.
- [15] L. Gonzlez, E. Siavichay, and J. Espinoza, "Impact of ev fast charging stations on the power distribution network of a latin american intermediate city," *Renewable and Sustainable Energy Reviews*, vol. 107, pp. 309 – 318, 2019.
- [16] K. Qian, C. Zhou, and Y. Yuan, "Impacts of high penetration level of fully electric vehicles charging loads on the thermal ageing of power transformers," *International Journal of Electrical Power & Energy Systems*, vol. 65, pp. 102 – 112, 2015.
- [17] R. Godina, E. Rodrigues, N. Paterakis, O. Erdinc, and J. Catalo, "Innovative impact assessment of electric vehicles charging loads on distribution transformers using real data," *Energy Conversion and Management*, vol. 120, pp. 206 – 216, 2016.
- [18] R. Abousleiman and R. Scholer, "Smart charging: System design and implementation for interaction between plug-in electric vehicles and the power grid," *IEEE Transactions on Transportation Electrification*, vol. 1, no. 1, pp. 18–25, June 2015.
- [19] S. F. Abdelsamad, W. G. Morsi, and T. S. Sidhu, "Probabilistic impact of transportation electrification on the loss-of-life of distribution transformers in the presence of rooftop solar photovoltaic," *IEEE Transactions on Sustainable Energy*, vol. 6, no. 4, pp. 1565–1573, Oct 2015.
- [20] J. Tan and L. Wang, "Adequacy assessment of power distribution network with large fleets of phev considering condition-dependent transformer faults," *IEEE Transactions on Smart Grid*, vol. 8, no. 2, pp. 598–608, March 2017.
- [21] S. Shokrzadeh, H. Ribberink, I. Rishmawi, and E. Entchev, "A simplified control algorithm for utilities to utilize plug-in electric vehicles to reduce distribution transformer overloading," *Energy*, vol. 133, pp. 1121 – 1131, 2017.
- [22] G. Razeghi, L. Zhang, T. Brown, and S. Samuelsen, "Impacts of plug-in hybrid electric vehicles on a residential transformer using stochastic and empirical analysis," *Journal of Power Sources*, vol. 252, pp. 277 – 285, 2014.
- [23] R. Godina, E. M. Rodrigues, J. C. Matias, and J. P. Catalo, "Smart electric vehicle charging scheduler for overloading prevention of an industry client power distribution transformer," *Applied Energy*, vol. 178, pp. 29 – 42, 2016.
- [24] C. M. Affonso and M. Kezunovic, "Technical and economic impact of pv-bess charging station on transformer life: A case study," *IEEE Transactions on Smart Grid*, pp. 1–1, 2018.
- [25] H. Ding, Z. Hu, and Y. Song, "Value of the energy storage system in an electric bus fast charging station," *Applied Energy*, vol. 157, pp. 630 – 639, 2015.
- [26] K. Chaudhari, N. K. Kandasamy, A. Krishnan, A. Ukil, and H. B. Gooi, "Agent-based aggregated behavior modeling for electric vehicle charging load," *IEEE Transactions on Industrial Informatics*, vol. 15, no. 2, pp. 856–868, Feb 2019.
- [27] Anti-Windup, "Integral Anti-Windup for PI Controllers, [Available Online]:<https://www.scribd.com/document/181677842/anti-windup>, [Accessed on: 2019-03-09]."
- [28] A. Visioli, "Modified anti-windup scheme for PID controllers," *IEE Proceedings - Control Theory and Applications*, vol. 150, no. 1, pp. 49–54, Jan 2003.
- [29] U. Datta, A. Kalam, and J. Shi, "Battery energy storage system control for mitigating pv penetration impact on primary frequency control and state-of-charge recovery," *IEEE Transactions on Sustainable Energy*, pp. 1–1, 2019.
- [30] V. Knap, S. K. Chaudhary, D. Stroe, M. Swierczynski, B. Craciun, and R. Teodorescu, "Sizing of an energy storage system for grid inertial response and primary frequency reserve," *IEEE Transactions on Power Systems*, vol. 31, no. 5, pp. 3447–3456, Sep. 2016.